Molecular Neurobiology (2019) 56:5856–5865
https://doi.org/10.1007/s12035-019-1476-7

JNK Isoforms Are Involved in the Control of Adult Hippocampal Neurogenesis in Mice, Both in Physiological Conditions and in an Experimental Model of Temporal Lobe Epilepsy

Rubén D. Castro-Torres[1,2,3] · Jon Landa[1] · Marina Rabaza[1] · Oriol Busquets[2,4,5,6] · Jordi Olloquequi[7] · Miren Ettcheto[2,4,5,6] · Carlos Beas-Zarate[3] · Jaume Folch[4,5] · Antoni Camins[2,5,6] · Carme Auladell[1,5,6] · Ester Verdaguer[1,5,6]

Received: 7 September 2018 / Accepted: 10 January 2019 / Published online: 26 January 2019

Abstract

Neurogenesis in the adult dentate gyrus (DG) of the hippocampus allows the continuous generation of new neurons. This cellular process can be disturbed under specific environmental conditions, such as epileptic seizures; however, the underlying mechanisms responsible for their control remain largely unknown. Although different studies have linked the JNK (c-Jun-N-terminal-kinase) activity with the regulation of cell proliferation and differentiation, the specific function of JNK in controlling adult hippocampal neurogenesis is not well known. The purpose of this study was to analyze the role of JNK isoforms (JNK1/JNK2/JNK3) in adult-hippocampal neurogenesis. To achieve this goal, we used JNK-knockout mice (*Jnk1*$^{-/-}$, *Jnk2*$^{-/-}$, and *Jnk3*$^{-/-}$), untreated and treated with intraperitoneal injections of kainic acid (KA), as an experimental model of epilepsy. In each condition, we identified cell subpopulations at different stages of neuronal maturation by immunohistochemical specific markers. In physiological conditions, we evidenced that JNK1 and JNK3 control the levels of one subtype of early progenitor cells (GFAP$^+$/Sox2$^+$) but not the GFAP$^+$/Nestin$^+$ cell subtype. Moreover, the absence of JNK1 induces an increase of immature neurons (Doublecortin$^+$; PSA-NCAM$^+$ cells) compared with wild-type (WT). On the other hand, *Jnk1*$^{-/-}$ and *Jnk3*$^{-/-}$ mice showed an increased capacity to maintain hippocampal homeostasis, since calbindin immunoreactivity is higher than in WT. An important fact is that, after KA injection, *Jnk1*$^{-/-}$ and *Jnk3*$^{-/-}$ mice show no increase in the different neurogenic cell subpopulation analyzed, in contrast to what occurs in WT and *Jnk2*$^{-/-}$ mice. All these data support that JNK isoforms are involved in the adult neurogenesis control.

Keywords JNK isoforms · Knockout mice · Adult hippocampal neurogenesis · Kainic acid

Carme Auladell and Ester Verdaguer contributed equally to this work.

Electronic supplementary material The online version of this article (https://doi.org/10.1007/s12035-019-1476-7) contains supplementary material, which is available to authorized users.

✉ Carme Auladell
cauladell@ub.edu

[1] Departament de Biologia Cellular, Fisiologia i Immunologia, Facultat de Biologia, Universitat de Barcelona, Barcelona, Spain

[2] Departament de Farmacologia, Toxicologia i Química Terapèutica, Facultat de Farmàcia i Ciències de l'Alimentació, Universitat de Barcelona, Barcelona, Spain

[3] Departamento de Biología Celular y Molecular, Laboratorio de Regeneración Neural, C.U.C.B.A, Universidad de Guadalajara, 44340 Jalisco, Mexico

[4] Departament de Bioquímica i Biotecnologia, Facultat de Medicina i Ciències de la Salut, Universitat Rovira i Virgili, Reus, Tarragona, Spain

[5] Networking Research Center on Neurodegenerative Diseases (CIBERNED), Instituto de Salud Carlos III, Madrid, Spain

[6] Institut de Neurociències, Universitat de Barcelona, Barcelona, Spain

[7] Facultad de Ciencias de la Salud, Universidad Autónoma de Chile, 5 Poniente No. 1670, 3460000 Talca, Chile

Abbreviations

ABC	avidin-biotin-peroxidase complex
CB	calbindin
CR	calretinin
CT	control
CBP	Calcium-binding protein
DAB	diaminobenzidine
DCX	doublecortin
DG	dentate gyrus
FBS	fetal bovine serum
GCL	granular cell layer
GC	granule cells
GFAP	glial fibrillary acidic protein
i.p	intraperitoneal injection
IR	immunoreactive
JNKs	c-Jun N-terminal kinases
JNK1, JNK2, and JNK3	JNK isoforms
jnk1	Knockout mice for JNK1
$jnk2^{-/-}$	knockout mice for JNK2
jnk3	knockout mice for JNK3
KA	kainic acid
KO	knockout
NSC	neural stem cells
O/N	overnight
PB	phosphate buffer
PBS	phosphate-buffered saline
PSA-NCAM	polysialic acid neural cell adhesion molecule
RT	room temperature
SD	standard deviation
SDA-PAGE	sodium dodecyl sulfate polyacrylamide gel electrophoresis.
SDS	sodium dodecyl sulfate
SEM	standard error of mean
SGZ	subgranular zone
TLE	temporal lobe epilepsy
WT	wild type

Introduction

The c-Jun N-terminal kinases (JNKs), a subfamily of the mitogen-activated protein kinases (MAPK), are stimulus-response proteins involved in a wide spectrum of cellular processes, including cell proliferation, differentiation, migration, inflammation, and apoptosis [1]. They are encoded by three genes in mammals: *Mapk8 (Jnk1)*, *Mapk9 (Jnk2)*, and *Mapk10 (Jnk3)*, which are expressed differentially in the brain [2]. The activation of JNKs is carried out by two MAPKs: MKK4 and MKK7 [3]. Once activated, JNK can translocate to the nucleus and control the expression of several transcriptional factors and nuclear hormone receptors [2, 4] or phosphorylate other non-nuclear substrates [5]. Moreover, different studies highlighted the important role of JNK in the pathogenesis of several diseases, such as diabetes, lung fibrosis, inflammatory and neurodegenerative disorders, and cancer [6]. Hence, understanding the function of the JNK pathway would be a major step towards developing specific therapeutic strategies for different diseases.

Elucidating the specific function of JNK isoforms is paramount in order to understand the complexity of JNK signaling. An approach to this analysis has been achieved studying JNK knockout (KO) mice ($Jnk1^{-/-}$, $Jnk2^{-/-}$, and $Jnk3^{-/-}$) [7–9]. Eventually, we know that JNK1 and JNK2 are probably essential in normal cell function and, presumably, they have redundant roles, since both show cooperative or synergistic effects [10]. Furthermore, it has been demonstrated that they participate in apoptosis regulation during normal brain development [11]. Nonetheless, specific functions have also been described for JNK1 and JNK2, such as the different and opposite effects on fibroblasts and macrophages proliferation [10, 12]. JNK1 and JNK2 differentially regulate T cell expansion during the viral lymphocytic choriomeningitis [13]. Moreover, $Jnk1^{-/-}$ mice showed greater abnormal cortical neuronal migration, anterior commissure degeneration during brain development [14], and disturbed metabolic regulation [15]. In addition, mice lacking JNK1, or treated with a JNK1 inhibitor (DJNKI-1), display an increased adult hippocampal neurogenesis [16]. Concerning $Jnk2^{-/-}$ mice, they show a less remarkable phenotype, with epidermal hyperplasia and mild immune abnormalities [10]. Lastly, JNK3 is clearly associated with neuronal death and oxidative stress. Thus, $Jnk3^{-/-}$ mice show a decrease in c-Jun phosphorylation in ischemia–hypoxia experimental models [17] and in cytochrome-c (cyt-c) release after spinal cord injury [18]. Furthermore, targeted disruption of *Jnk3* in mice confers a high resistance to kainic acid (KA), an analogue of glutamic acid that has been used to establish excitotoxicity models in vitro and in vivo [8, 19, 20]. KA induces an enhancement of neurogenesis in the dentate gyrus (DG) of the hippocampus by promoting hippocampal hyperexcitability [21], a pathological feature in patients with mesial temporal lobe epilepsy (TLE) [22–25]. In this regard, we have recently demonstrated that $Jnk1^{-/-}$ mice also show neuroprotection against KA, as previously described in $Jnk3^{-/-}$ mice [9, 19].

Specifically, the adult hippocampal neurogenesis in DG occurs in an intermittent zone between the granular cell layer (GCL) and the hilus, called the subgranular zone (SGZ), where a continuous generation of new neurons takes place [26]. These new cells originate from neural stem cells (NSCs) and are structurally integrated into the network of mature granule cells (GCs). This cellular process plays an important role in hippocampal functions related to learning and memory, as well as in mood regulation [27]. Therefore, disturbances in their activity may lead, in addition to epilepsy, to serious cognitive disorders, such as dementia and depression [28, 29].

The aim of the present study was to analyze the role of each JNK isoform (JNK1, JNK2, and JNK3) in the control of hippocampal neurogenesis, both in physiological conditions and under the toxicity of KA. To achieve this goal, we used JNK KO mice (*Jnk1*$^{-/-}$, *Jnk2*$^{-/-}$, and *Jnk3*$^{-/-}$), untreated and treated with intraperitoneal injections of KA. In each condition, we identified cell subpopulations in the SGZ at different stages of neuronal maturation. We determined these subpopulations with the use of specific biomarkers: (i) GFAP (glial fibrillary acidic protein), Nestin protein (neuroectodermal stem cell marker), a type of intermediate filament and Sox2 (transcription factor, SRY-like homeobox 2) which detects NSC or early precursors cells (type 1), (ii) doublecortin (DCX) and polysialic acid-neural cell adhesion molecule (PSA-NCAM), two proteins that target transit-amplifying progenitor cells or immature neurons (types 2a and 2b), and (iii) calretinin (CR), a calcium binding protein (CBP) that helps to identify neuroblasts, which represent the last stage of neuron precursor development (type 3). Since new CR-positive cells modify their expression from CR to calbindin (CB) as they integrate into the existing network, [30], we analyzed the distribution pattern of CB immunoreactive cells in hippocampal areas.

Materials and Methods

Animals

Two-month-old C57BL/6 wild-type (WT) and KO mice for the JNKs isoforms (*jnk1*$^{-/-}$, *jnk2*$^{-/-}$, *jnk3*$^{-/-}$) were used in this study. The generation and characterization of *jnk1*$^{-/-}$, *jnk2*$^{-/-}$, and *jnk3*$^{-/-}$ single knockout mice have been previously described [7–9]. Mice were backcrossed to the C57BL/6 genetic background. Throughout the experiments, all mice were housed in a controlled environment, and food and water were available ad libitum. The experiments were conducted in accordance with the Council of Europe Directive 2010/63. The procedure was registered at the *Department d'Agricultura, Ramaderia i Pesca* of the *Generalitat de Catalunya*. Ref. Number order 8852.

Kainic Acid Treatment and Sample Processing

Animals were divided into two treatments: (i) single intraperitoneal (i.p.) dose (30 mg/kg) of KA (Sigma-Aldrich, USA) dissolved in 0.9% saline and (ii) single i.p. dose of 0.9% saline solution (control group; CT) [31]. After 24 h, mice were anesthetized by i.p. administration of pentobarbital (80 mg/kg) and were perfused with paraformaldehyde (40 g/L) diluted in 0.1 mol/L phosphate buffer (PB). Brains were removed and post-fixed with the same fixative for 24 h; subsequently, they were transferred into the same solution enriched with 300 g/L sucrose for 24 h. Finally, brain samples were frozen to obtain coronal sections of 20 μm in a cryostat (Leica Microsystems, Wetzlar, Germany). Free-floating samples were kept in a cryoprotectant in the freezer until use.

Finally, the following eight experimental groups were established: WT CT, WT KA, *Jnk1*$^{-/-}$ CT, *Jnk1*$^{-/-}$ KA, *Jnk2*$^{-/-}$ CT, *Jnk2*$^{-/-}$ KA, *Jnk3*$^{-/-}$ CT, and *Jnk3*$^{-/-}$ KA.

Immunofluorescences

The primary antibodies used for immunofluorescences were mouse anti-Nestin antibody (1:200, MAB353, Millipore), rabbit anti-Sox2 (1:500, ab97959, Abcam), goat anti-DCX (1:200, sc-8066, Santa Cruz Biotechnology), mouse anti-PSA-NCAM (1:1000, ABC Scientific), rabbit anti-NeuN (1:500, 24307, Cell Signal Technology), rabbit anti-GFAP (1:1000, Z0334, DAKO), and mouse anti-GFAP (1:1000, M0761, DAKO). The secondary antibodies used were donkey anti-goat Alexa 488, goat anti-mouse Alexa 594, goat anti-mouse Alexa 488; goat anti-rabbit Alexa 594, and goat anti-rabbit Alexa 488 (1:200, Life Technology).

Free-floating sections were rinsed in PBS, pH 7.2 prior to pre-incubation in a blocking solution (10% of fetal bovine serum (FBS), 1% of triton X-100 in phosphate-buffered saline (PBS) at room temperature 1 h. Then, they were incubated overnight (O/N) at 4 °C with the corresponding primary antibody and 2 h for the corresponding secondary antibody. We reported two single immunofluorescences against DCX and PSA-NCAM, and three double immunofluorescences against Sox2/GFAP, Nestin/GFAP, and PSA-NCAM/NeuN. The incubation of the primary and secondary antibodies was performed sequentially. At the end, sections were counterstained with 0.1 μg/mL Hoechst 33258 (Sigma-Aldrich, USA) for nuclear stains during 10 min in the dark. Immediately after that, samples were rinsed with PBS and were mounted onto gelatinized slides with Fluoromount medium (Sigma-Aldrich, USA). Stained sections were examined under an epifluorescence microscope (Olympus BX61).

Inmunohistochemistry

The primary antibodies used for enzymatic immunohistochemistry were goat anti-DCX (1:200, sc-8066, Santa Cruz Biotechnology), rabbit anti-Calbindin (1:1000) (Swant Inc., Switzerland), and rabbit anti-Calretinin (1:1000; Swant Inc., Switzerland). Biotinylated secondary antibody horse anti-goat (1:200, Vector Labs), goat anti-rabbit (1:200; Sigma, St. Louis, MO, USA), and horse anti-rabbit (1:200; Sigma-Aldrich, USA) were used.

Enzymatic immunohistochemistry was performed using free-floating technique [31]. First, the sections were rinsed in 0.1 M PB, pH 7.2, and treated with 3% H_2O_2 and 1% methanol in PBS to inactivate endogenous peroxidase for 15 min and then were incubated with the blocking solution as

previously described. Then, they were incubated overnight (O/N) at 4 °C with the corresponding primary antibody and 2 h for the corresponding secondary antibody. After that, the avidin–biotin–peroxidase complex (ABC, Vector Laboratories, USA) was used to develop the chromogenic reaction with 0.05% diaminobenzidine (DAB) in 0.1 M PB and 0.005% H_2O_2. For a double enzymatic immunohistochemistry, a second round of incubation of primary and secondary and ABC complex was performed developing chromogenic reaction using 0.05% DAB-0 with 0.005% H_2O_2, 0.05% cobalt chloride, and 0.05% nickel ammonium sulfate. We reported a single immunohistochemistry against calbidin and a double against calretinin/DCX.

Counting of Immunoreactive Cells

Sections corresponding to the hippocampal levels between Bergman −1.28 and −2.12 mm, in accordance with the Atlas reported by Paxinos et al. [32], were used to perform the cell counting of SGZ of the DG (four to six animals/genotype and age, four to eight sections/animal). In each hippocampus, two field of ×20 magnification were used to count visually spanning from apex towars to the infra and supragranular layers of the dentate gyrus in a total area of 844 × 317.8 μm^2. Then, we report the cell counting as a normalized values per counting area.

Statistical Analysis

All data are presented in box plot graph using the median as the center value; the ends of the box are the lower and upper quartiles, and the ends of the whiskers as minimum and maximum values. The level of significance was fixed at $\alpha = 0.05$. Statistical analyses across the experimental groups were evaluated using individual value per counting area from each animal and performing one-way ANOVA followed by a Holm-Šídák post hoc test for multiple comparisons. Both statistical analyses and graphs were created with the GraphPad InStat software V5.0 (GraphPad Software Inc., San Diego, CA, USA).

Results

Differential Response of Early Precursor Cells (Nestin$^+$/GFAP$^+$ and Sox2$^+$/GFAP$^+$), in Physiological Conditions and After KA Treatment

The analyses of early precursor cells (type 1) were obtained through double immunofluorescence assays, such as GFAP and Nestin protein and GFAP and Sox2, as a markers of radial glia-like neural stem cells NSC [33, 34].

Nestin$^+$/GFAP$^+$ Cell Progenitors

The levels of GFAP$^+$/Nestin$^+$ radial glia-like cells in the SGZ of the hippocampus were similar among JNK KOs CT and WT CT animals (Fig. 1a, b). However, after 24 h of KA injection, this subpopulation, located in the SGZ, increased in WT and *Jnk2*$^{-/-}$ mice compared with their controls (Fig. 1a, b), whereas no change was detected in *Jnk1*$^{-/-}$ and *Jnk3*$^{-/-}$ mice (Fig. 1a, b).

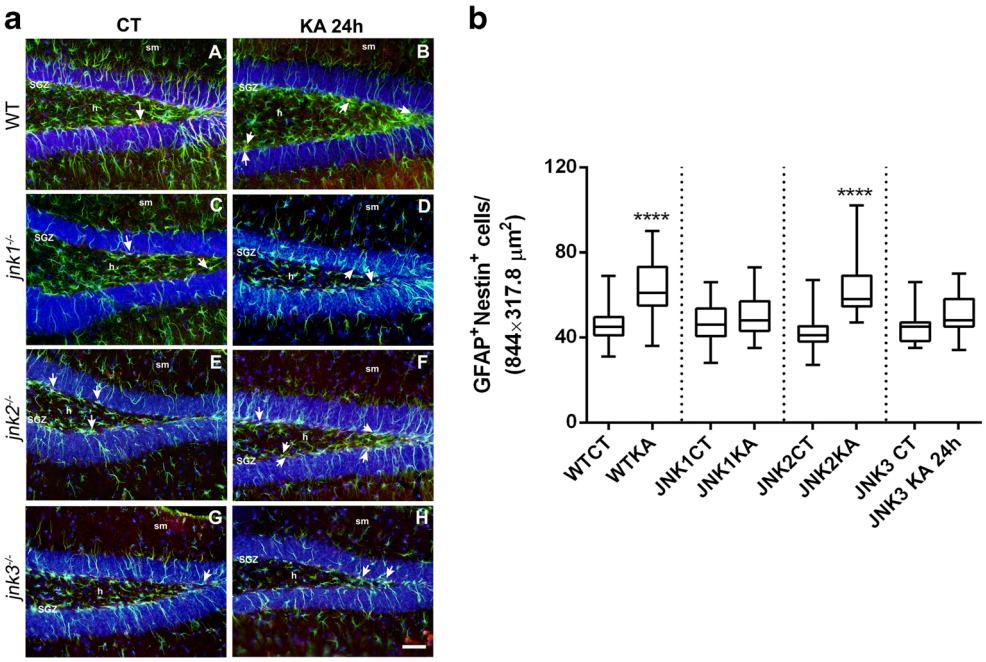

Fig. 1 **a** Representative DG hippocampal images of GFAP/Nestin immunofluorescence (green and red, respectively), from control mice (*A*, *C*, *E*, *G*) and 24 h KA-treated mice (*B*, *D*, *F*, *H*) of WT, *jnk1*$^{-/-}$, *jnk2*$^{-/-}$, and *jnk3*$^{-/-}$. Arrows show double immunofluorescence cells. **b** Quantification of the number of GFAP/Nestin-positive cells and the representative histogram. ****$P > 0.0001$ vs WT CT SGZ: subgranular zone; h: hilus; sm: stratum moleculare. Scale bar 50 μm

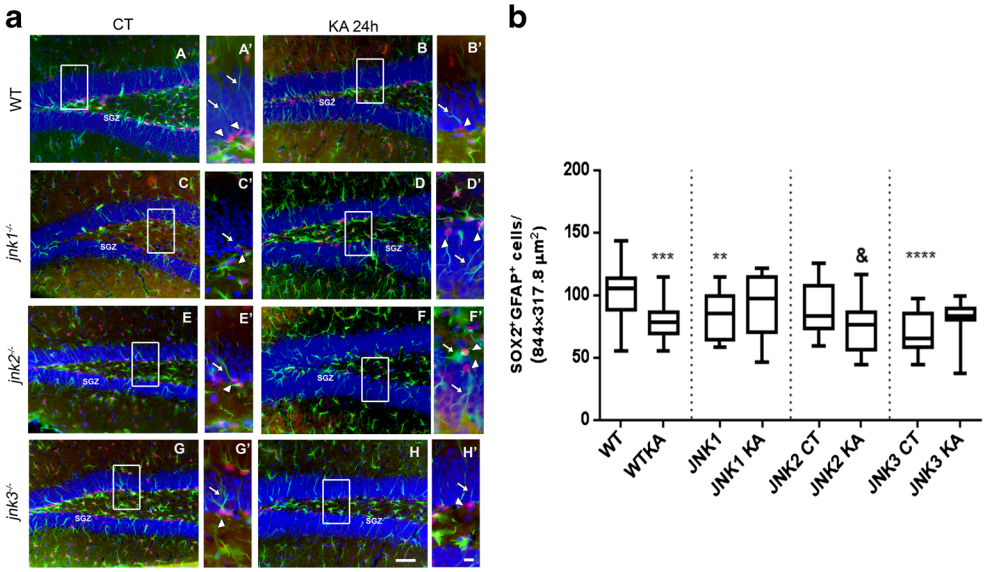

Fig. 2 **a** Representative DG hippocampal images of GFAP/Sox2 immunofluorescence (green and red, respectively), from control mice (*A*, *C*, *E*, *G*) and 24 h KA-treated mice (*B*, *D*, *F*, *H*) of WT, *jnk1*$^{-/-}$, *jnk2*$^{-/-}$, and *jnk3*$^{-/-}$. A′–H′ show high magnification of double-labeled cells. Arrows indicate the cellular processes of radial glia-like cells immunopositive for GFAP; arrowheads signal their nuclei. **b** Quantification of the number of GFAP-Sox2-positive cells and the representative histogram. $^{**}P < 0.01$, $^{***}P < 0.001$, and $^{****}P < 0.0001$ vs WT CT;; $^{\&}P < 0.05$ vs genotype control. SGZ: subgranular zone. *A–H* Scale bar 50 µm, A′–H′ scale bar 10 µm

GFAP$^+$/Sox2$^+$ Cell Progenitors

In physiological conditions, the number of GFAP$^+$/Sox2$^+$ cells was lower in *Jnk1*$^{-/-}$ and *Jnk3*$^{-/-}$ mice compared with WT CT (Fig. 2a, b). By contrast, there were no differences between WT CT and *Jnk2*$^{-/-}$ CT mice (Fig. 2a, b). After KA injection, a decrease of GFAP$^+$/Sox2$^+$ cells was observed in WT KA compared with WT CT and in *Jnk2*$^{-/-}$ KA versus *Jnk2*$^{-/-}$ CT (Fig. 2a, b).

The high co-localization of GFAP, Sox2, and Nestin hinders the quantification of single immunolabeled Sox2$^+$ or Nestin$^+$ radial glia-like cells. These populations represent a very low pool of cells, and they were unable to quantify with certainty. Further studies should be conducted to clarify the role of these pools of cell in epilepsy.

The Absence of JNK1 Induces an Increase in the Number of Immature Neurons, in Physiological Conditions

DCX Cell Transit-Amplifying Cells

DCX is a microtubule-associated protein expressed in the transiently amplifying progenitor cells and immature neurons (types 2a and 2b) of the adult brain, specifically in areas of continuous neurogenesis [35]. The immunofluorescence against DCX revealed that the number of DCX$^+$ cells in *Jnk1*$^{-/-}$ CT mice was higher than in WT CT (Fig. 3a, b). No differences were detected in *Jnk2*$^{-/-}$ CT and *Jnk3*$^{-/-}$ CT mice compared with WT CT (Fig. 3a, b). After KA treatment, the levels of DCX$^+$ increased in WT mice compared with their CT (Fig. 3a, b). No significant changes were observed in *Jnk1*$^{-/-}$, *Jnk2*$^{-/-}$, and *Jnk3*$^{-/-}$ mice after KA injection compared to their controls (Fig. 3a, b).

In order to identify a more differentiated neuronal cell subpopulation, a co-immunolabeling of DCX and CR was performed. Interestingly, we found high levels of double-positive DCX$^+$/CR$^+$ cells in all genotypes; however, few numbers of single immunolabel DCX$^+$ cells were found (Fig. 4). Moreover, this immunostaining allowed the identification of at least two cellular phenotypes in physiological conditions: (i) cells with positive staining for DCX in plasma membrane and dendritic projections, and double DCX and CR staining in soma (Fig. 4), and (ii) cells with soma exclusively stained for CR however with still DCX stain in dendritic projections. The first DCX$^+$-CR$^+$ cell subtype was mainly located in the SGZ. In physiological conditions, these cells were significantly increased in *Jnk1*$^{-/-}$ CT mice and decreased in *Jnk3*$^{-/-}$ CT mice compared to WT CT (Fig. 4 and Fig. S1). Regarding *Jnk2*$^{-/-}$ CT mice, no difference in the number of these cells was observed when compared to WT CT (Fig. S1). After KA treatment, only WT and *Jnk2*$^{-/-}$ mice showed changes in these cell numbers; however, while an increase was observed in WT (Fig. 4 and Fig. S1), a decrease was detected in *Jnk2*$^{-/-}$ mice (Fig.4 and Fig. S1). No effect was detected in *Jnk1*$^{-/-}$ and *Jnk3*$^{-/-}$ treated mice relative to their CT (Fig. S1). In addition, double immunostaining also showed alterations in the dendritic pattern in all JNK KO CT mice compared to WT CT (Fig. 4). Moreover, the soma of DCX$^+$/CR$^+$ cells in *Jnk3*$^{-/-}$ CT mice was clearly distorted when compared to WT CT (Fig.

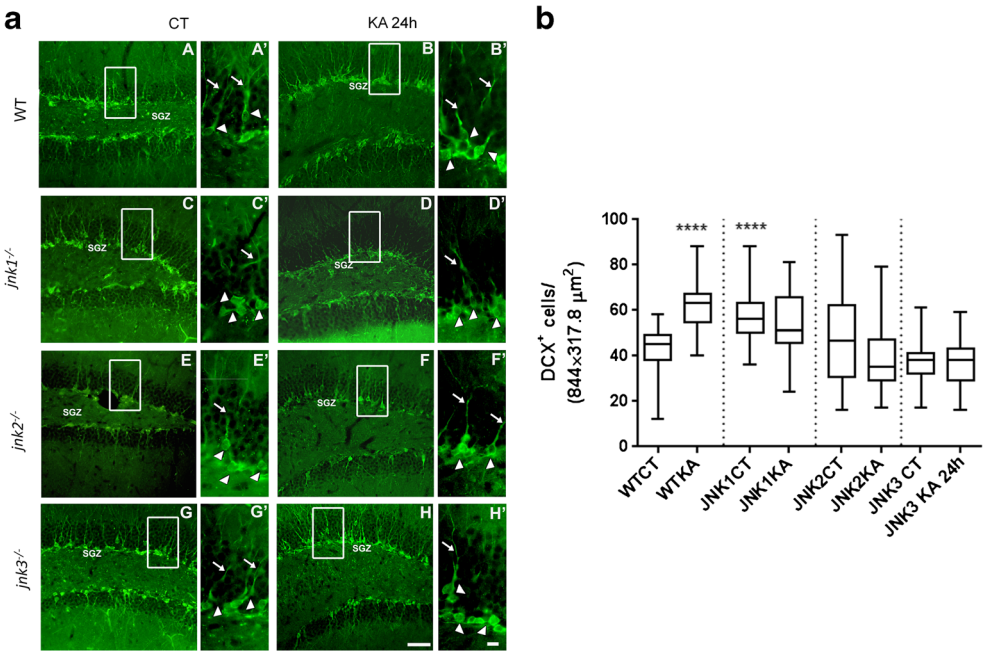

Fig. 3 **a** Representative DG hippocampal images of Doublecortin (DCX) immunofluorescence, from control mice (*A*, *C*, *E*, *G*) and after 24 h of KA injections (*B*, *D*, *F*, *H*). *A*, *B* WT; C-D: *Jnk1*$^{-/-}$; *E*, *F* *Jnk2*$^{-/-}$; *G*, *H* *Jnk3*$^{-/-}$. A detail of DCX-IR cells is shown in panels (A′–H′). The arrows indicate the cell projections and the arrowhead their soma. **b** Bar graphs represent the number of DCX-positive cell and the representative histogram. *P < 0.05, **P < 0.01, and ***P < 0.0001 vs WT CT and $^{\&}P$ < 0.05 vs genotype control. SGZ: subgranular zone. *A*–*H* Scale bar 50 µm. A′–H′ Scale bar 10 µm

4). Regarding the second DCX$^+$/CR$^+$ cell subtype, it was mainly located above the SGZ, specifically in the granular cell layer (GCL) (Fig. 4).

Most of the second subtype of DCX$^+$/CR$^+$ cells were located above the SGZ, in the granular cell layer (GCL) (Fig. 4).

PSA-NCAM Cell Transit-Amplifying Cells

PSA-NCAM plays a role in regulating processes such as migration, survival, and outgrowth of newly generated neurons [36]. The distribution pattern of PSA-NCAM$^+$ cells was the same as

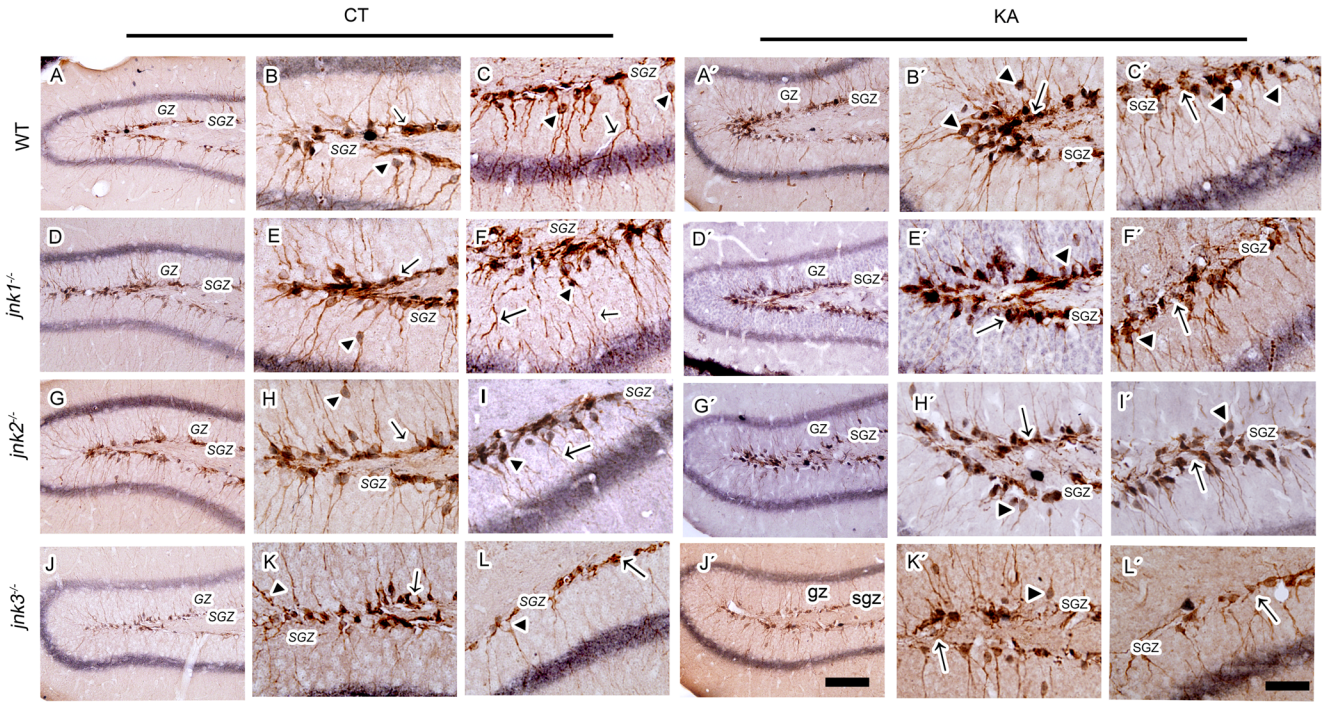

Fig. 4 Representative DG hippocampal images of double immunohistochemistry Doublecortin-calretinin (DCX$^+$/CR$^+$), from control mice (**A**–**L**) and 24 h KA-treated mice (A′–L′) of WT, *jnk1*$^{-/-}$, *jnk2*$^{-/-}$, and *jnk3*$^{-/-}$. WT. D–F′ *Jnk1*$^{-/-}$; G–I′ *Jnk2*$^{-/-}$; J–L′ *Jnk3*$^{-/-}$. Arrowheads mark the soma of cells immunopositive for CR, and arrows the projections immunopositive for DCX. SGZ: subgranular zone; gz: granular zone. Scale bar 50 µm

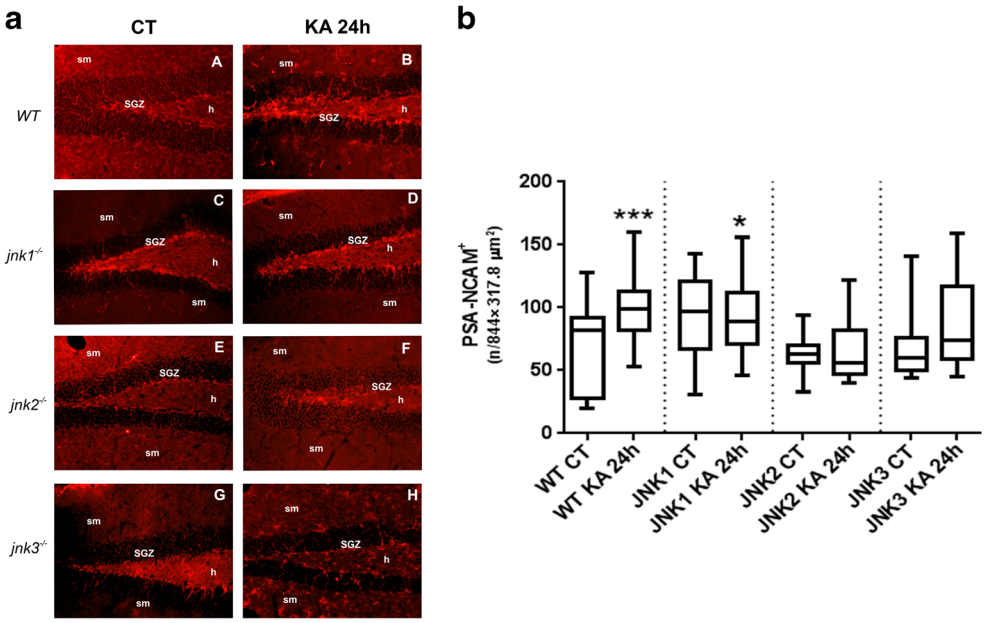

Fig. 5 **a** Representative DG hippocampal images of PSA-NCAM immunopositive cells, obtained from control mice (*A*, *C*, *E*, *G*) and 24 h KA-treated mice (*B*, *D*, *F*, *H*) of WT, *jnk1*$^{-/-}$, *jnk2*$^{-/-}$, and *jnk3*$^{-/-}$ mice. *A*, *B* WT; *C*, *D* *Jnk1*$^{-/-}$; *E*, *F* *Jnk2*$^{-/-}$; *G*, *H* *Jnk3*$^{-/-}$. **b** Graphs represent the number of PSA-NCAM-positive cells in SGZ. *$P < 0.05$, ***$P < 0.0001$ vs WT CT. SGZ: subgranular zone, h: hilus; sm: stratum moleculare. Scale bar 50 µm

the one observed for DCX$^+$ cells. Thus, the number of PSA-NCAM$^+$ cells was higher in *Jnk1*$^{-/-}$ CT mice than in WT CT (Fig. 5a, b). After KA injection, an increase in PSA-NCAM$^+$ cells was observed in WT mice (Fig. 5a, b) and no changes in cell levels were observed in any JNK knockouts mice (Fig. 5b).

In order to identify more differentiated transit-amplifying cells, we performed a double immunostaining for PSA-NCAM and NeuN. This last protein is a nuclear antigen, commonly used as a marker for mature neurons [37, 38]. The counting of PSA-NCAM$^+$/NeuN$^+$ cells evidenced that their number was low in all genotypes (Fig. S2). In addition, no significant differences were observed in JNK KOs compared to WT CT, in physiological conditions. After KA injection, an increase of PSA-NCAM$^+$/NeuN$^+$ cells were observed only in WT CT (Fig. S2).

Calbindin Immunoreactivity Was Higher in *Jnk1*$^{-/-}$ and *Jnk3*$^{-/-}$ Mice than in WT and *Jnk2*$^{-/-}$ Mice, in Physiological Conditions

Mature granule cells in the adult DG are known to express calbindin [39]. Our results revealed higher immunoreactivity in *Jnk1*$^{-/-}$ and *Jnk3*$^{-/-}$ CT mice compared with WT CT (Fig. 6). The immunostaining intensity was slightly lower in *Jnk2*$^{-/-}$ CT mice (Fig. 6). Finally, after KA injection, there

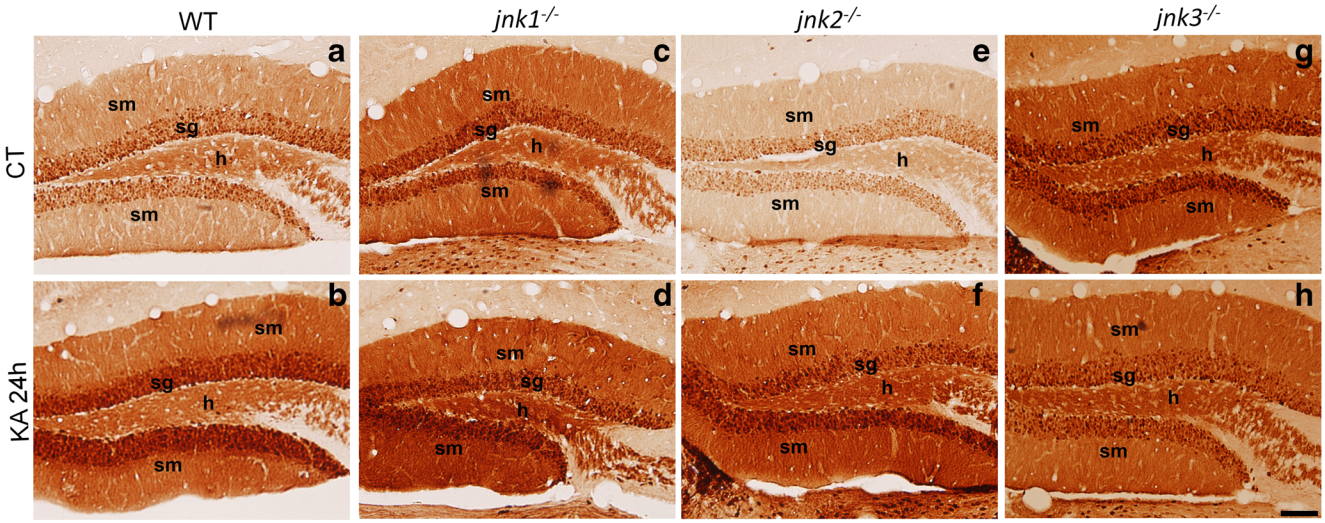

Fig. 6 Calbindin immunofluorescence distribution pattern in the DG of hippocampal coronal sections, obtained from control mice (**a**, **c**, **e**, **g**) and after 24 h of KA injections (**b**, **d**, **f**, **h**). **a**, **b** WT; **c**, **d** *Jnk1*$^{-/-}$; **e**, **f** *Jnk2*$^{-/-}$; **g**, **h** *Jnk3*$^{-/-}$. ZSG: subgranular zone; h: hilus; sm: stratum moleculare. Scale bar 100 µm

was an increase in immunoreactivity in WT mice (GCL layer) and *Jnk2*$^{-/-}$ mice (GCL and hilus) (Fig. 6) but not in *Jnk1*$^{-/-}$ and *Jnk3*$^{-/-}$ mice (Fig. 6).

Discussion

The objective of this study was to evaluate how the absence of JNK isoforms affects the number and the distribution pattern of different neuronal precursor cell subpopulations on the DG, in physiological conditions and in mice treated with KA.

Early Progenitor Cells In physiological conditions, the absence of JNK isoforms has no effect on the levels of GFAP$^+$/Nestin$^+$ cells, compared with WT CT; however, the levels of GFAP$^+$/Sox2$^+$ cells decrease with the lack of JNK1 and JNK3 with respect to WT CT. After KA injection, *Jnk1*$^{-/-}$ and *Jnk3*$^{-/-}$ mice have no changes in the number of these cell subtypes with respect to their controls, in contrast with what occurs in WT and *Jnk2*$^{-/-}$ mice, which shows an increase in the number of GFAP$^+$/Nestin$^+$ cells and a decrease in GFAP$^+$/Sox2$^+$ cells.

Transit Amplifying Cells In physiological conditions, the levels of DCX$^+$ and PSA-NCAM$^+$ cells increase with the absence of JNK1, compared with WT CT, while no changes are observed with the lack of JNK2 and JNK3 isoforms. The effect of KA to these cell types is observed only in WT.

The Lack of JNK Isoforms Has a Different Control in Distinct Early Progenitor Cells

Two subtypes of early progenitor cells were analyzed (GFAP/Nestin and GFAP/Sox2), and high levels of co-localization among biomarkers were detected. Thus, we only analyzed the distribution pattern of the double-labeled cells (GFAP$^+$/Nestin$^+$ and GFAP$^+$/Sox2$^+$). In physiological conditions, the results evidenced that JNKs have a different control among these subpopulations. While no JNK isoforms control the levels of GFAP$^+$/Nestin$^+$ cells, the JNK1 and JNK3 isoforms are involved in the regulation of GFAP$^+$/Sox2$^+$ cell levels.

Following KA injection, the examination of these cell subtypes stated that only the lack of JNK2 induces the same changes that are observed in WT. The interesting point is that both subpopulations responded differentially to KA. While an increase was observed in GFAP$^+$/Nestin$^+$ cells, a decrease was visualized in GFAP$^+$/Sox2$^+$ cells.

These results reveal that both subtypes of early progenitor cells are differentially regulated, suggesting that or pointing at that there are cell progenitors of different cell lineages.

The Lack of JNK1 Isoform and JNK3 Prevent Alterations of Neurogenic Cell Subpopulations after KA

In physiological conditions, the transit-amplifying cells (DCX$^+$, DCX$^+$-CR$^+$, and PSA-NCAM$^+$) increase in mice that lack the JNK1 isoform. Thus, the rate of proliferation in *Jnk1*$^{-/-}$ CT mice is higher than in WT CT. These data are in accordance with those reported by Mohammad et al. [16], who showed that mice lacking JNK1, or mice treated with a JNK inhibitor (DJNKI-1), display increased neurogenesis in the hippocampus. Considering that the levels of early progenitor cells (GFAP$^+$/Nestin$^+$ and GFAP$^+$/Sox2$^+$) in adult *Jnk1*$^{-/-}$ mice, in physiological conditions, are lower or equal to WT CT, the higher levels of immature neurons (neuroblasts) in adult *Jnk1*$^{-/-}$ mice, compared to WT CT, could be due to an accumulation of these cells in the SGZ. This can be due to an alteration in their migration into the granular cell layer. It is known that the JNK pathway is linked to the reelin pathway that regulates cortical layering [40]. Moreover, it has been recently described that there are new neuroblasts formed during embryonic development, retained in quiescent state during postnatal period until to be reactivated [41].

Despite this increase in immature neurons in *Jnk1*$^{-/-}$ mice, they have neuroprotection against KA [19]. These data are in accordance with Iyengar et al. [42], who selectively removed newborn neurons and found increased susceptibility to the convulsing effects of KA. By contrast, Cho et al. [43] demonstrated that the ablation of neurogenesis does not affect seizures severity in an animal model treated with pilocarpine. Taking all these data into consideration, we can infer that the neuroprotection in *Jnk1*$^{-/-}$ mice is due to unchanged levels of the different neurogenic cell subtypes after KA, compared to their CT. This effect seems important, because it also occurs in *Jnk3*$^{-/-}$ mice that likewise prevents neurodegeneration or shows neuroprotection against KA [19] and, in physiological conditions, *Jnk3*$^{-/-}$ mice show a reduction in neurogenesis activity, with a significant value in DCX$^+$/CR$^+$ cell subtypes, in comparison with WT CT. Taking into consideration the results of Dominguez et al. [39] who suggest that the rise observed in WT mice, after KA, is due to the existence of a reservoir of pre-existing, not completely differentiated, granule cells, instead of being a direct product of neurogenesis, it is plausible that in *Jnk1*$^{-/-}$ and *Jnk3*$^{-/-}$ mice, the effect of KA is not able to achieve the activation of this reservoir pool, preserving the brain damage induced with this neurotoxin.

The DCX/CR double immunostaining allowed the identification of high co-localization between DCX and CR. This can be explained by the existence of different subtypes of DCX/CR-immunolabeled cells. Thus, the neuronal maturation must be gradual and associated to differences in the amount of proteins. In consequence, the cells with exclusive CR staining in soma but still DCX staining

in dendrites could be the ones that migrate radially into the GCL. The dendritic outgrowth and neuronal motility of these cells justify the presence of DCX in their dendrites [44]. In addition, it is known that CR is transiently expressed and, when it disappears, the expression of CB, which marks the switch to adult-like connectivity in granular cells, starts [45] being difficult to detect cells exclusively immunoreactive to CR.

The data obtained with the double immunostain (DCX/CR), together with the low number of PSA-NCAM$^+$/NeuN$^+$ subtype cells detected, suggest that the transition from transit-amplifying cells to immature neurons takes a long time, and in contrast, the passage to differentiated neuron is faster. All these data could explain why finding a single CR$^+$ or PSA-NCAM$^+$/NeuN$^+$ cell is difficult.

Another data reported with the double immunostaining (DCX/CR) is that the absence of JNK isoforms induces alterations in the dendritic pattern of immature neurons. Hence, all the JNKs take part in the dendritic maturation, without compensatory effects between isoforms, as it is described in brain morphogenesis and axodendritic architecture during development [46]. Therefore, JNKs are involved in the morphology control of cells located in the SGZ and in their neurogenic rate.

CB is a CBP present in mature granule cells that acts as a modulator of calcium homeostasis, calcium channel activity, and neuronal plasticity [30, 47]. Therefore, the high levels of CB-IR in *Jnk1*$^{-/-}$ and *Jnk3*$^{-/-}$ mice suggest that they have more capacity to control homeostasis than WT and *Jnk2*$^{-/-}$ CT mice.

In conclusion, the present study shows that *Jnk1*$^{-/-}$ and *Jnk3*$^{-/-}$ CT mice have an enhanced hippocampal homeostasis when compared to WT CT and *Jnk2*$^{-/-}$ CT mice. Moreover, the lack of JNK1 or JNK3 induces different neurogenesis activity in the SGZ, under physiological conditions, but in both genotypes, the increase in early progenitor cells and immature neurons after KA is prevented, and consequently interrupted one of the pathological features of TLE, whereas the absence of JNK2 preserves the increase in immature neurons which does not preserve the alterations in early progenitor cells.

All these findings justify the development of selective inhibitors for JNK1 and JNK3 in order to develop drugs with neuroprotective and cognitive effects.

Acknowledgements This work was supported by Ministerio Español de Ciencia e Innovación, SAF2017-84283-R; Centro de Investigación Biomédica en Red de Enfermedades Neurodegenerativas (CIBERNED) CB06/05/0024; Consejo Nacional de Ciéncia y Tecnologia, CONACYT, 177594; Generalitat de Catalunya, 2014SGR-525; Generalitat de Catalunya, 2017 SGR 625; Postdoctoral Fellowship CONACYT-MEXICO, 298337; Doctoral Program in Sciences in Molecular Biology in Medicine LGAC; and Molecular Bases of Chronic-Degenerative Diseases and its Applications 000091, PNPC, CONACYT-MEXICO.

Thanks to Kyra -Mae Leighton for her technical support.

References

1. Davis RJ (2000) Signal transduction by the JNK group of MAP kinases. Cell 103:239–252
2. Gupta S, Barrett T, Whitmarsh a J et al (1996) Selective interaction of JNK protein kinase isoforms with transcription factors. EMBO J 15:2760–2770
3. Ip YT, Davis RJ (1998) Signal transduction by the c-Jun N-terminal kinase (JNK)–from inflammation to development. Curr Opin Cell Biol 10:205–219
4. Karin M (1995) The regulation of AP-1 activity by mitogen-activated protein kinases. J Biol Chem 270:16483–16486. https://doi.org/10.1098/rstb.1996.0008
5. Bogoyevitch MA, Kobe B (2006) Uses for JNK: the many and varied substrates of the c-Jun N-terminal kinases. Microbiol Mol Biol Rev 70:1061–1095. https://doi.org/10.1128/MMBR.00025-06
6. Gkouveris I, Nikitakis NG (2017) Role of JNK signaling in oral cancer: a mini review. Tumor Biol 39:101042831771165
7. Dong C, Yang DD, Wysk M, Whitmarsh AJ, Davis RJ, Flavell RA (1998) Defective T cell differentiation in the absence of Jnk1. Science 282:2092–2095. https://doi.org/10.1126/science.282.5396.2092
8. Yang DD, Conze D, Whitmarsh AJ et al (1998) Differentiation of CD4+ T cells to Th1 cells requires MAP kinase JNK2. Immunity 9:575–585
9. Yang DD, Kuan CY, Whitmarsh a J et al (1997) Absence of excitotoxicity-induced apoptosis in the hippocampus of mice lacking the Jnk3 gene. Nature 389:865–870. https://doi.org/10.1038/39899
10. Zeke A, Misheva M, Reményi A, Bogoyevitch MA (2016) JNK signaling: regulation and functions based on complex protein-protein partnerships. Microbiol Mol Biol Rev 80:793–835. https://doi.org/10.1128/MMBR.00043-14
11. Kuan CY, Yang DD, Samanta Roy DR et al (1999) The Jnk1 and Jnk2 protein kinases are required for regional specific apoptosis during early brain development. Neuron 22:667–676
12. Sabapathy K (2012) Role of the JNK pathway in human diseases. Prog Mol Biol Transl Sci 106:145–169
13. Conze D, Krahl T, Kennedy N, Weiss L, Lumsden J, Hess P, Flavell RA, le Gros G et al (2002) c-Jun NH(2)-terminal kinase (JNK)1 and JNK2 have distinct roles in CD8(+) T cell activation. J Exp Med 195:811–823. https://doi.org/10.1084/JEM.20011508
14. Myers AK, Meechan DW, Adney DR, Tucker ES (2014) Cortical interneurons require Jnk1 to enter and navigate the developing cerebral cortex. J Neurosci 34:7787–7801. https://doi.org/10.1523/JNEUROSCI.4695-13.2014
15. Hirosumi J, Tuncman G, Chang L, Görgün CZ, Uysal KT, Maeda K, Karin M, Hotamisligil GS (2002) A central role for JNK in obesity and insulin resistance. Nature 420:333–336. https://doi.org/10.1038/nature01137
16. Mohammad H, Marchisella F, Ortega-Martinez S, Hollos P, Eerola K, Komulainen E, Kulesskaya N, Freemantle E et al (2018) JNK1 controls adult hippocampal neurogenesis and imposes cell-autonomous control of anxiety behaviour from the neurogenic niche. Mol Psychiatry 23:487. https://doi.org/10.1038/mp.2017.21
17. Kuan C-Y, Whitmarsh AJ, Yang DD, Liao G, Schloemer AJ, Dong C, Bao J, Banasiak KJ et al (2003) A critical role of neural-specific JNK3 for ischemic apoptosis. Proc Natl Acad Sci U S A 100:15184–15189. https://doi.org/10.1073/pnas.2336254100
18. Li QM, Tep C, Yune TY, Zhou XZ, Uchida T, Lu KP, Yoon SO (2007) Opposite regulation of oligodendrocyte apoptosis by JNK3

and Pin1 after spinal cord injury. J Neurosci 27:8395–8404. https://doi.org/10.1523/JNEUROSCI.2478-07.2007

19. de Lemos L, Junyent F, Camins A, Castro-Torres RD, Folch J, Olloquequi J, Beas-Zarate C, Verdaguer E et al (2017) Neuroprotective effects of the absence of JNK1 or JNK3 isoforms on kainic acid-induced temporal lobe epilepsy-like symptoms. Mol Neurobiol. https://doi.org/10.1007/s12035-017-0669-1
20. De Lemos L, Junyent F, Verdaguer E et al (2010) Differences in activation of ERK1/2 and p38 kinase in Jnk3 null mice following KA treatment. J Neurochem 114:1315–1322. https://doi.org/10.1111/j.1471-4159.2010.06853.x
21. Raijmakers M, Clynen E, Smisdom N, Nelissen S, Brône B, Rigo JM, Hoogland G, Swijsen A (2016) Experimental febrile seizures increase dendritic complexity of newborn dentate granule cells. Epilepsia 57:717–726. https://doi.org/10.1111/epi.13357
22. Ben-Ari Y, Cossart R (2000) Kainate, a double agent that generates seizures: two decades of progress. Trends Neurosci 23:580–587. https://doi.org/10.1016/S0166-2236(00)01659-3
23. Parent JM (2003) Injury-induced neurogenesis in the adult mammalian brain. Neurosci 9:261–272. https://doi.org/10.1177/1073858403252680
24. Shetty AK, Hattiangady B, Rao MS, Shuai B (2012) Neurogenesis response of middle-aged hippocampus to acute seizure activity. PLoS One 7:e43286. https://doi.org/10.1371/journal.pone.0043286
25. Sakurai M, Suzuki H, Tomita N, Sunden Y, Shimada A, Miyata H, Morita T (2017) Enhanced neurogenesis and possible synaptic reorganization in the piriform cortex of adult rat following kainic acid-induced status epilepticus. Neuropathology 38:135–143. https://doi.org/10.1111/neup.12445
26. Walton RM (2012) Postnatal neurogenesis. Vet Pathol 49:155–165. https://doi.org/10.1177/0300985811414035
27. Kempermann G, Song H, Gage FH (2015) Neurogenesis in the adult hippocampus. Cold Spring Harb Perspect Biol 7:a018812. https://doi.org/10.1101/cshperspect.a018812
28. Zhao C, Deng W, Gage FH (2008) Mechanisms and functional implications of adult neurogenesis. Cell 132:645–660. https://doi.org/10.1016/j.cell.2008.01.033
29. Braun SMG, Jessberger S (2014) Review: adult neurogenesis and its role in neuropsychiatric disease, brain repair and normal brain function. Neuropathol Appl Neurobiol 40:3–12. https://doi.org/10.1111/nan.12107
30. Brandt MD, Jessberger S, Steiner B, Kronenberg G, Reuter K, Bick-Sander A, Behrens W, Kempermann G (2003) Transient calretinin expression defines early postmitotic step of neuronal differentiation in adult hippocampal neurogenesis of mice. Mol Cell Neurosci 24:603–613. https://doi.org/10.1016/S1044-7431(03)00207-0
31. Junyent F, Utrera J, Romero R, Pallàs M, Camins A, Duque D, Auladell C (2009) Prevention of epilepsy by taurine treatments in mice experimental model. J Neurosci Res 87:1500–1508. https://doi.org/10.1002/jnr.21950
32. Paxinos G, Franlin K (2012) The mouse brain in stereotaxic coordinates, 4th edn. Academic Press
33. Zhang J, Jiao J (2015) Molecular biomarkers for embryonic and adult neural stem cell and neurogenesis. Biomed Res Int 2015: 727542–727514. https://doi.org/10.1155/2015/727542
34. Brazel CY, Limke TL, Osborne JK, Miura T, Cai J, Pevny L, Rao MS (2005) Sox2 expression defines a heterogeneous population of neurosphere-forming cells in the adult murine brain. Aging Cell 4: 197–207. https://doi.org/10.1111/j.1474-9726.2005.00158.x
35. Couillard-Despres S, Winner B, Schaubeck S, Aigner R, Vroemen M, Weidner N, Bogdahn U, Winkler J et al (2005) Doublecortin expression levels in adult brain reflect neurogenesis. Eur J Neurosci 21:1–14. https://doi.org/10.1111/j.1460-9568.2004.03813.x
36. Gascon E, Vutskits L, Kiss JZ (2010) The role of PSA-NCAM in adult neurogenesis. Springer, New York, pp. 127–136
37. Mullen RJ, Buck CR, Smith AM (1992) NeuN, a neuronal specific nuclear protein in vertebrates. Development 116:201–211
38. Seki T, Arai Y (1993) Distribution and possible roles of the highly polysialylated neural cell adhesion molecule (NCAM-H) in the developing and adult central nervous system. Neurosci Res 17:265–290
39. Domínguez MI, Blasco-Ibáñez JM, Crespo C et al (2003) Calretinin/PSA-NCAM immunoreactive granule cells after hippocampal damage produced by kainic acid and DEDTC treatment in mouse. Brain Res 966:206–217. https://doi.org/10.1016/S0006-8993(02)04164-1
40. Reiner O, Gdalyahu A, Ghosh I et al (2004) DCX's phosphorylation by not just another kinase (JNK). Cell Cycle 3:747–751
41. Pino A, Fumagalli G, Bifari F, Decimo I (2017) New neurons in adult brain: distribution, molecular mechanisms and therapies. Biochem Pharmacol 141:4–22. https://doi.org/10.1016/j.bcp.2017.07.003
42. Iyengar SS, LaFrancois JJ, Friedman D et al (2015) Suppression of adult neurogenesis increases the acute effects of kainic acid. Exp Neurol 264:135–149. https://doi.org/10.1016/j.expneurol.2014.11.009
43. Cho K-O, Lybrand ZR, Ito N, Brulet R, Tafacory F, Zhang L, Good L, Ure K et al (2015) Aberrant hippocampal neurogenesis contributes to epilepsy and associated cognitive decline. Nat Commun 6: 6606. https://doi.org/10.1038/ncomms7606
44. Gdalyahu A, Ghosh I, Levy T, Sapir T, Sapoznik S, Fishler Y, Azoulai D, Reiner O (2004) DCX, a new mediator of the JNK pathway. EMBO J 23:823–832. https://doi.org/10.1038/sj.emboj.7600079
45. Todkar K, Scotti AL, Schwaller B (2012) Absence of the calcium-binding protein calretinin, not of calbindin D-28k, causes a permanent impairment of murine adult hippocampal neurogenesis. Front Mol Neurosci 5(56). https://doi.org/10.3389/fnmol.2012.00056
46. Coffey ET (2014) Nuclear and cytosolic JNK signalling in neurons. Nat Rev Neurosci 15:285–299. https://doi.org/10.1038/nrn3729
47. Lledo PM, Somasundaram B, Morton AJ, Emson PC, Mason WT (1992) Stable transfection of calbindin-D28k into the GH3 cell line alters calcium currents and intracellular calcium homeostasis. Neuron 9:943–954